JCI The Journal of Clinical Investigation

Notch signaling dynamically regulates adult β cell proliferation and maturity

Alberto Bartolome, … , Lori Sussel, Utpal B. Pajvani

J Clin Invest. 2018. https://doi.org/10.1172/JCI98098.

Research In-Press Preview **Endocrinology** **Metabolism**

Graphical abstract

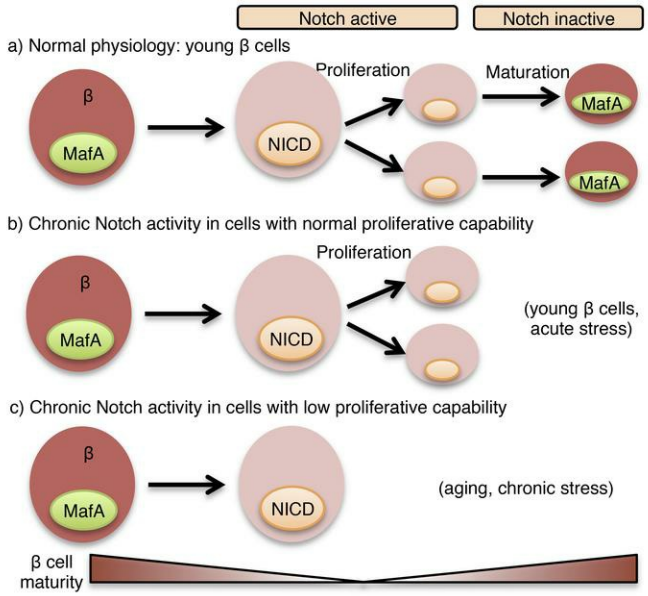

Notch signaling dynamically regulates adult β cell proliferation and maturity

Alberto Bartolome[1], Changyu Zhu[1], Lori Sussel[2] and Utpal B. Pajvani[1]

[1]Department of Medicine, Columbia University, New York, NY, USA

[2]Department of Pediatrics, University of Colorado, Denver, CO, USA

Correspondence should be addressed to U. B. P (up2104@columbia.edu)

Full address: Columbia University Medical Center. Russ Berrie Science Pavilion.

1150 St. Nicholas Avenue. New York, NY 10032

Phone: +1-212-851-4886

Conflict of interest statement: The authors have declared that no conflict of interest exists.

ABSTRACT

Notch signaling regulates differentiation of the pancreatic endocrine lineage during embryogenesis, but the role of Notch in mature β cells is unclear. We found that islets derived from lean mice show modest β cell Notch activity, which increases in obesity and in response to high glucose. This response appeared maladaptive, as mice with β cell-specific deficient Notch transcriptional activity (β-Rbpj, β-DNMAML) showed improved glucose tolerance when subjected to high-fat diet feeding. Conversely, mice with β cell-specific expression of constitutively-active Notch1 (β-NICD) had a progressive loss of β cell maturity, due to proteasomal degradation of MafA, leading to impaired glucose-stimulated insulin secretion and glucose intolerance with aging or obesity. Surprisingly, Notch-active β cells had increased proliferative capacity, leading to increased but dysfunctional β cell mass. These studies demonstrate a dynamic role for Notch in developed β cells to simultaneously regulate β cell function and proliferation.

KEYWORDS

Notch, beta cell, proliferation, maturity, MafA

INTRODUCTION

β cell mass and function adapts to the insulin requirements of the organism to maintain euglycemia across a wide range of pathophysiology, such as insulin resistance, pregnancy or aging (1). Molecular mechanisms that enable β cell adaptation to these stressors are not yet fully understood; insufficient functional adaptation, including β cell death and dedifferentiation, becomes clinically apparent with the onset of Type 2 Diabetes (T2D) (2, 3). With the continued increase in obesity, novel therapeutically-tractable pathways that regulate β cell adaptation are sought to reverse β cell dysfunction in T2D.

Notch mediates cell-fate decisions via juxtacrine interactions between neighboring cells expressing Notch receptors (Notch1-4) and ligands (Jagged1/2, Dll1/3/4). Mice lacking the common transcriptional effector of all Notch signaling, *Rbpj*, or other Notch pathway components are embryonically lethal, but even prior to lethality, Notch mutant mice showed abnormal pancreata (4, 5). In fact, both Notch gain- or loss-of-function impaired β cell differentiation (6, 7), underscoring the necessity of Notch signaling for normal development, but the potential role of Notch in the adult endocrine pancreas remained mostly unexplored, surprising with the subsequent identification of *NOTCH2* as a T2D susceptibility locus (8).

We have recently shown that liver Notch activity is increased in diet-induced obese mouse models and in T2D patients (9), and contributes to excess hepatic glucose production and fatty acid synthesis (10, 11). These data led us to hypothesize that Notch may be similarly reactivated in the stressed β cell, consistent with other “developmental” pathways in the dedifferentiated β cell (3). Here, we find that Notch signaling is present at low levels in fully developed β cells, but increased in islets cultured in hyperglycemic conditions or isolated from obese mice. Persistent β cell Notch signaling appears detrimental to function, as forced Notch activation impaired glucose-stimulated insulin secretion (GSIS) in isolated mouse or human islets, and glucose intolerance in β cell-specific Notch gain-of-function mouse models. Conversely, we observed improved glucose tolerance with genetic inhibition of β cell Notch

action. Mechanistically, we found that Notch interfered with MafA-Kat2b association, which induced MafA proteasomal degradation, loss of β cell maturity and surprisingly, a simultaneous β cell proliferative response. These data suggest that Notch signaling acts as a switch controlling two diametrically opposed events – maturity and proliferation – in adult β cells.

RESULTS

Notch signaling is dynamically regulated in developed pancreatic β cells

As a first step to evaluating a potential post-development role of β cell Notch signaling, we determined the absolute expression of Notch signaling components in islets isolated from wild type (WT) adult mice (Supplemental Figure 1A). This analysis revealed relatively high expression level of Notch receptors/ligands in islets, consistent with prevalent Rbpj staining in β cells (Figure 1A), suggesting potential for ongoing β cell Notch signaling. To assess Notch activation in the adult pancreas, we used Transgenic Notch Reporter (TNR) mice that express GFP under the control of a *Rbpj*-consensus sequence (12). Chow-fed TNR mice showed readily detectable Notch activity in a subset of β cells (Figure 1B), but trivial staining in other islet endocrine cells (Supplemental Figure 1B). We also observed an enrichment of β cell transcripts (i.e. *Ins2*) in FACS-sorted, Notch-active GFP+ islet cells (Supplemental Figure 1C). We next used another Notch reporter mouse model, with a more persistent fluorescent reporter (Histone2b-Venus) (13), to confirm these data – integrating both data sets, we find the islet Notch activity is essentially confined to β cells (Supplemental Figure 1D), but at generally lower levels than Notch activity detected in endothelial or duct cells (Supplemental Figure 1E), consistent with earlier observations (14).

We next evaluated whether β cell Notch activity was regulated by metabolic stimuli. We used low-dose streptozotocin (STZ) treatment to render TNR mice hyperglycemic, which increased β cell Notch activity (Figures 1C and Supplemental Figure 1F). This was confirmed by increased expression of the canonical Notch target, *Hes1*, in the surviving β cell population (Figure 1D). We attributed increased Notch activity to hyperglycemia, as opposed to an STZ-induced injury response, as high glucose exposure also resulted in increased GFP protein levels and *Hes1* expression in isolated TNR islets (Figures 1E and 1F), consistent with increased Notch signaling in islets from hyperglycemic NOD mice (15). Similarly, we found higher expression of *Hes1* and other Notch transcriptional targets in islets isolated from diet-

induced obese (DIO) mice as compared with chow-fed mice (Figure 1G), which corresponded with increased β cell Hes1 staining (Figure 1H). Thus, we conclude that Notch signaling is active in adult β cells, and enhanced in conditions associated with increased insulin demand (obesity, partial ablation of β cell mass, and hyperglycemia).

β cell Notch activation impairs GSIS, leading to glucose intolerance

To test whether Notch may contribute to β cell dysfunction, we generated β cell-specific Notch gain-of-function (β-NICD) mice by crossing *Rosa26-NICD* (7) with *RIP-Cre* (16) transgenic lines. Despite unchanged body weight (Supplemental Figure 2A), chow-fed β-NICD mice were mildly glucose intolerant as compared to Cre- controls (Figure 2A). These differences were exacerbated by aging (Figure 2B) or HFD feeding (Figure 2C), but completely reversed with simultaneous *Rbpj* deletion (Figure 2D), suggesting glucose intolerance was mediated by canonical Notch signaling. β-NICD mice showed unchanged fasting insulin levels (Supplemental Figure 2B), but blunted in vivo (Figure 2E) and ex vivo (Figure 2F) GSIS and a small decrease of total insulin content (Figure 2G). Consistent with this observation, islets from β-NICD mice showed decreased expression of genes corresponding to the GSIS machinery, including *Pcsk1, Pcsk2* and *Slc30a8* (Figure 2H), lower Slc2a2 staining (Figure 2I) and fewer β cell mature dense core insulin granules (Figure 2J).

To exclude impact of Notch activation during the early postnatal period, we generated tamoxifen (TAM)-dependent, β cell-specific (17) Notch gain-of-function (MIP-β-NICD) mice. MIP-β-NICD mice were indistinguishable from controls before TAM treatment, but consistent with data from β-NICD mice, showed increased glucose excursion after TAM treatment which was exacerbated by HFD-feeding (Supplemental Figure 2C). In sum, these data suggest that forced Notch activation in fully developed β cells is sufficient to impair functional response to obesity-induced insulin resistance.

Notch activity leads to a specific loss of β cell MafA in mouse and human islets.

To determine how Notch affects β cell function, we took a candidate approach focusing initially on key transcriptional regulators of GSIS such as Pdx1, MafA, and Nkx6.1. Of these, we found a profound reduction in MafA staining in pancreatic sections, islets and primary β cells from β-NICD and TAM treated MIP-β-NICD mice (Figures 3A, 3B and Supplemental Figure 3A, B), but importantly, not in β-NICD:Rbpj mice (Supplemental Figure 3C). Notch-mediated loss of β cell MafA appeared relatively specific, without effects on Pdx1 or Nkx6.1 (Figure 3C, Supplemental Figure 3D and not shown), and also did not lead to a compensatory response in MafB, which localizes in glucagon+ cells equally in control and β-NICD mice (Supplemental Figure 3E-F). Consistent with the hypothesis that decreased MafA is the mechanism of impaired GSIS with β cell Notch activation, shRNA-mediated *Mafa* silencing failed to exacerbate Notch inhibition of GSIS (Supplemental Figure 3G). Finally, NICD transduction in human islets also resulted in loss of MAFA (Figure 3D) and impaired GSIS (Figure 3E), as well as lower PDX1, but without changes in MAFB and NKX6.1 (Supplemental Figure 4A-C).

Notch causes MafA degradation by preventing its association with Kat2b.

Intriguingly, Notch activation reduced MafA protein without affecting *Mafa* expression (Supplemental Figures 5A and 5B), suggesting a post-transcriptional effect. To test this hypothesis, we generated a stable MIN6 line to allow doxycycline-dependent expression of a Notch1 gain-of-function mutant (N1ΔE) that does not require ligand binding but still requires γ-secretase processing to render NICD (18). As hypothesized, N1ΔE led to loss of MafA (Figure 3F), but not in the presence of a gamma-secretase inhibitor (GSI) (Supplemental Figures 5C and 5D) or in cells that express dominant-negative Mastermind-like1 (DNMAML), that inhibits function of the MAML transcriptional coactivator essential for Rbpj-dependent Notch signaling (Supplemental Figure 5E). Using this model, we confirmed that acute Notch activation rapidly decreases MafA protein (Figure 3G), without change in *Mafa* mRNA (Figure 3H).

We next observed that MG132-mediated proteasome inhibition preserved MafA protein levels (Figure 4A), which led us to hypothesize that Notch increases GSK3β activity, known to trigger MafA proteasomal degradation (19, 20). N1ΔE, however, did not affect GSK3β activation (Supplemental Figure 5F), although GSK3β inhibition prevented Notch mediated MafA ubiquitination (Supplemental Figure 5G) and degradation (Supplemental Figure 5H). Similarly, whereas exogenous MafA is also degraded with Notch activation, the GSK3β-resistant MafA-S65A mutant (21) is protected from Notch-induced degradation (Supplemental Figure 5I). These results suggest that Notch-induced proteasomal degradation of MafA is downstream of GSK3β-mediated phosphorylation.

The histone acetyltransferase Kat2b has been reported to protect MafA from proteasomal degradation in cancer cells (20); as Kat2b can also interact with NICD (22), we hypothesized that Notch may affect MafA-Kat2b interaction, leading to MafA degradation. Indeed, Notch activation prevented normal Kat2b-MafA association (Figure 4B), and Kat2b overexpression of in MIN6 cells protected MafA from Notch-mediated degradation (Figure 4C). Conversely, *Kat2b* silencing in MIN6 cells induced loss of MafA (Figures 4D and 4E) without changing *Mafa* expression (Supplemental Figure 5J), and recapitulated the impaired GSIS associated with Notch activation (Figure 4F). In sum, these data show that Notch disrupts MafA-Kat2b interaction, which induces MafA proteasomal degradation and impaired β cell function (Figure 4G).

Notch activation and reduced maturity in proliferating β cells

Profiling experiments have reported reduced gene expression of maturity markers in proliferating β cells (23). In line with this idea, we observed lower MafA protein in BrdU+ cells from WT pregnant females (Figure 5A and Supplemental Figure 6A), but normal Pdx1, NeuroD1 or Ucn3 (Figure 5B). We found a similar effect in MIN6 cells, which lose MafA when undergoing chromatin condensation prior to cell division, but retain Pdx1 and Nkx6.1 (Supplemental Figure

6B). Consistent with a Notch-MafA axis to regulate β cell maturity and proliferation, we observed increased Notch-active β cells in pregnant females as compared to virgin females (Figure 5C), as well as in the highly proliferative β cells remaining post-STZ treatment (Figure 1C-D and Supplemental Figure 6C). In fact, the population of KI67+ proliferating β cells in pregnant TNR mice is enriched in GFP+ cells (Figure 5D); consistently, MafA levels are modestly reduced in GFP+ cells (Figure 5E).

These results suggest that a transient increase in Notch activity accompanies loss of β cell maturity in the course of normal β cell self-replication. We next asked whether persistent Notch activation causes loss of β cell maturity – indeed, islets from β-NICD mice showed a transcriptional signature of immaturity (decreased *Mafa, Glp1r, Ucn3* and increased *Ldha*, Supplemental Figures 6D and 6E). Similar data were observed in TAM treated MIP-β-NICD mice (Supplemental Figure 6F). Reduced *Mafa* and maturity in Notch-active β cells could arise from a feed-forward loop of Maf-transcription factors (24), as previously shown for *Mafa* (25), or that chronic metabolic abnormalities in Notch gain-of-function mice repressed *Mafa*. To distinguish these possibilities, we treated islets derived from MIP-β-NICD mice with chronic 4-hydroxytamoxifen (4-OHT)-treatment, which also revealed reduced *Mafa* (Supplemental Figures 6G and 6H). In sum, these data indicate that β cell Notch activation destabilizes MafA which, in turn, represses the β cell maturation program but does not result in complete loss of cell identity, as lineage-tracing experiments did not reveal β cell transdifferentiation or dedifferentiation in β-NICD mice (Supplemental Figure 6I).

Notch induces β cell proliferation, leading to increased β cell mass

The positive correlation between Notch activity and β cell proliferation in TNR mice led us to test causation. We observed an increase in β cell mass of β-NICD mice, due to a shift towards larger islet size (Figure 6A and Supplementary Figure 7A). We attributed increased β cell mass in β-NICD mice to increased β cell proliferation (Figures 6B and 6C), detectable as early as

postnatal day 14 (P14) (Figure 6D), as β cell death was unchanged (Supplemental Figure 7B). β cell mass remained higher in β-NICD mice even at 1 year of life (Figure 6E), when β cell proliferation rates were low and not different from control mice (Supplemental Figure 7C), suggesting that Notch-induced β cell mass acquisition may be maintained through adulthood.

To determine necessity of intact Notch signaling for proliferation, we generated β cell specific Notch loss-of-function (β-DNMAML) mice which showed decreased β cell proliferation at P14 (Figure 6F). To establish whether Notch regulation of beta cell proliferation was cell-autonomous, we isolated islets from MIP-β-NICD and MIP-β-DNMAML mice, then treated with 4-OHT to induce recombination. Consistent with in vivo results, forced Notch activation increased glucose-induced proliferation, while genetic blockade of β cell Notch activation reduced proliferation (Figure 6G and Supplemental Figure 7D). Importantly, we observed unchanged proliferation capacity when cells were cultured in low glucose, where proliferation rate remains low (Supplemental Figure 7E). Similarly, Notch gain-of-function enhanced proliferation during pregnancy (Figure 6H), whereas pregnancy-induced β cell proliferation was diminished in Notch loss-of-function mice (Figure 6I). We conclude from these results that endogenous Notch activation augments β cell proliferation in times of need, but simultaneously suggest that Notch is neither necessary nor sufficient to force proliferation-incompetent (i.e. aging, low-glucose growth conditions) β cells to divide.

β cell Notch inhibition improves obesity-induced glucose intolerance.

We next circled back to our original observations, and hypothesized that blocking Notch signaling in β cells may increase MafA stability, and improve obesity-induced glucose intolerance. Indeed, expression of DNMAML reversed loss of MafA seen in primary β cells challenged with high glucose and palmitate (Figure 7A). Consistently, DNMAML increased the half-life of exogenous MafA in cycloheximide-treated MIN6 cells (Figure 7B).

To test whether β cell-specific Notch loss-of-function could reverse loss of MafA in HFD-fed mice (Supplemental Figures 8A and 8B), we utilized MIP-β-DNMAML mice but delayed TAM-induced recombination and HFD-feeding until mid-adulthood (Supplemental Figure 8C), to both bypass the β cell proliferation differences attributable to Notch in the early postnatal period and minimize the proliferative effect of human growth hormone (hGH) minigene in the MIP-Cre^{ERT} transgene (26, 27). We confirmed the utility of this strategy, as WT and MIP-Cre^{ERT} mice (without floxed alleles) showed similar glucose tolerance, body weight, β cell proliferation and β cell mass when HFD-feeding was initiated at 24 weeks of life (Supplemental Figures 8D-8G), in contrast to MIP-Cre^{ERT} mice fed HFD when β cells are more proliferative (26). With this experimental paradigm, MIP-β-DNMAML mice demonstrated improved glucose tolerance (Figure 7C). As predicted, islets from these mice showed lower Notch activity (Supplemental Figure 8H), but also indications of greater β cell maturity (Figure 7D and 7E).

To ensure reproducibility, we created a second, inducible Notch loss-of-function mouse model, MIP-β-Rbpj mice, which showed normal glucose tolerance when fed chow diet (Supplemental Figure 8I), but improved glucose tolerance as compared to Cre- controls when challenged with HFD feeding (Figure 7F). Consistent with data from MIP-β-DNMAML mice, islets from MIP-β-Rbpj mice had decreased Notch activation (Supplemental Figure 8J), with a parallel increase in MafA levels, leading to a pro-maturity β cell expression profile (Figures 7I and 7J). Finally, as predicted given the delay in HFD-induced insulin resistance until β cells are less proliferative, both Notch loss-of-function models showed unchanged β cell mass or β cell proliferation from Cre- controls, and thus unchanged fasted serum insulin levels (Supplemental Figures 8I-8K and not shown). These data indicate that Notch inhibition stabilizes MafA, leading to increased β cell maturity and improved glucose tolerance in the face of obesity-induced metabolic challenge.

DISCUSSION

Reactivation of “embryonic” signaling pathways can occur in environmentally stressed β cells (3). For instance, increased Notch signaling has been shown in hypoxia (28) or when islets are compromised in the setting of pericyte ablation (29). Since these same stressors also lead to β cell dysfunction, cause and effect cannot be disentangled, but here we show that unrestrained Notch activation is detrimental to β cell maturity and leads to disrupted GSIS in isolated mouse and human islets, as well as impaired glucose tolerance in vivo in conditions associated with increased systemic demand for insulin. Reciprocally, genetic inhibition of Notch activation maintains β cell function when mice are challenged by HFD-feeding, independent of Notch’s well-established role in pancreatic endocrine development (6, 7, 30).

Our data also indicate that constitutive Notch activation cannot induce dedifferentiation, unlike forced activation of Hedgehog signaling (31), nor is Notch activation sufficient to trigger β cell replication, but rather leads to higher proliferative rate in conditions associated with β cell division. These data suggest that Notch activation pushes stressed β cells further away from *status quo*, but whether the positive effect of Notch signaling on β cell proliferation is a direct consequence of Notch activation, a byproduct of loss of β cell maturity or both is not yet known. These findings do however support the idea of β cell function being opposed to β cell proliferation (32), and a model where the proliferating population of β cells is both Notch-active and functionally immature, with a readout of destabilized MafA. These data are consistent with in vitro work showing Notch activation in proliferating human β cells (33, 34), as well as studies on proliferating β cells in vivo (23), which showed repression of the Pdx1/NeuroD1/MafA network, but not gene expression of these canonical β cell transcription factors, or loss of other maturity markers such as Ucn3 (35). Of these, MafA has been consistently shown to be essential for β cell function and survival in the adult pancreas (36-38). Various circumstantial data suggests that partial loss of MafA activity may represent commitment to β cell division – 1) forced MafA expression in pancreatic progenitors increased expression of cell cycle inhibitors

and blunted cell proliferation (39); 2) MafA only becomes essential for β cell function after weaning (36); and 3) *MafA* expression is low during the postnatal proliferative wave (40), and in hyperproliferative human insulinomas with altered *MENIN* expression (41). However, total ablation of MafA in whole body or pancreas-specific knockout models does not result in hyperproliferative β cells – on the contrary, loss of β cell mass was reported (36, 38). One possible explanation – that loss of MafA may lead to compensatory MafB expression, reported to mediate β cell proliferative adaptation to pregnancy (42, 43) and β cell maturation (44, 45) – did not hold true in Notch-active β cells. This may indicate that dynamic regulation of MafA activity is required for normal regulation of β cell maturity and proliferation, perhaps by Notch effects on Kat2b-MafA interaction. Thus, our data are broadly consistent with the protective role of MafA for β cell adaption to stress (46-48), but further studies are necessary to test MafA-dependence on Notch's various effects on β cell biology, as well as to determine Kat2b interaction partners in β cells in various pathophysiologic states.

We observe heterogeneous Notch activation in β cells, consistent with differential proliferative capability of distinct β cell populations (49, 50); in fact, the proliferative "bottom β cell population" identified by Rui and colleagues shows increased *Hes1* expression (50). Notch activation is at minimum a readout of this β cell heterogeneity, but likely accounts for variability in cell-to-cell MafA and resultant propensity to proliferate. Although we have not yet identified the source of the Notch signal, our preliminary data point to β cell specific upregulation of specific Notch ligands of the Delta-like and Jagged families in response to hyperglycemia, which suggest the possibility of stressed β cells sending out a call for proliferation. But our data cannot exclude other endocrine or non-endocrine signal-sending cells; similarly, as our Notch loss-of-function mouse models focused on common downstream signaling components (MAML, Rbpj), future studies will be necessary to identify the specific Notch receptor activated in β cells.

In sum, we find active Notch signaling in the "normal" β cell, but with two disparate outcomes: in young mice, Notch activation represents an adaptive mechanism to increase β cell

mass induced by insulin resistance, by permissive action on proliferation; but in aged mice with lower proliferative capability (51), or with chronic insults, such as obesity, Notch activation locks β cells into an immature and dysfunctional state – a maladaptive compensatory response. Thus, Notch loss-of-function enhances β cell maturity and improves glucose tolerance. These data parallel findings in liver (9) and other insulin-sensitive tissues (52, 53) where similar Notch "reactivation" is causal to insulin resistance (10, 11, 54-56). As Notch is therapeutically accessible (57), with small molecules and biologics in the pipeline for cancer (58), these results provide the groundwork to repurpose these agents to address the dual pathologies – insulin resistance and deficient insulin secretion – that characterize T2D.

METHODS

Animals

RIP-Cre: Tg(Ins2-cre)23Herr (16)*, MIP-Cre^{ERT}: B6.Cg-Tg(Ins1-cre/ERT)1Lphi/J* (17)*, R26-NICD*: *Gt(ROSA)26Sor$^{tm1(Notch1)Dam}$* (7)*, R26-DNMAML1: Gt(ROSA)26Sor$^{tm1.1(Maml1/EGFP)Hri}$* (59) and *Rbpj fl/fl*: *Rbp^{jtm1Hon}* (6) mouse lines were maintained on a C57BL/6J background. Transgenic Notch Reporter: *Tg(Cp-EGFP)25Gaia/ReyaJ* (TNR) mice were maintained in homozygosity to avoid epigenetic silencing on a C57BL/6J and SJL/J mixed background (12). H2B-Venus Notch Reporter: *Tg(Cp-HIST1H2BB/Venus)47Hadj* were maintained in homozygosity on a FVB background (13). Mice were weaned and maintained on standard chow (Purina Mills no. 5053) or HFD (Harlan Laboratories TD.06414) as stated. Adult mice (8-12 weeks old) were used for experiments, unless stated otherwise. No differences in body weight or glucose tolerance were found between wild type and *RIP-Cre* or *MIP-Cre^{ERT}* mice (not shown). Male mice were used for all experiments described, with the exception of experiments involving pregnancy, and ex vivo GSIS where islets from mice and female mice were used without distinction.

Antibodies and chemicals

All antibodies used can be found in Supplemental Table 1. STZ, tamoxifen, 4-hydroxytamoxifen, doxycycline hyclate, MG132, cycloheximide, BrdU and LiCl were obtained from Millipore-Sigma. CHIR 99021 was obtained from Tocris Bioscience.

STZ and tamoxifen treatment

STZ was dissolved in cold citrate buffer 0.1M pH 4.5, and injected within 10-15 minutes of preparation, once daily at a dose of 50 mg STZ/kg body weight for five consecutive days. Mice were sacrificed 18 days after last STZ injection, with fed glucose levels 450-520 mg/dl. Tamoxifen was dissolved in corn oil (Millipore-Sigma) and sterile-filtered; both Cre- controls and

CreERT+ mice were treated with 100 mg tamoxifen/kg body weight once daily for 3 consecutive days.

Islet Isolation

Islets were routinely isolated by collagenase P (Roche Applied Science) digestion of whole pancreas (except for electron microscopy experiments), followed by Histopaque density-gradient centrifugation as described (60). When required, islets were maintained ex vivo in 5.5 mM glucose RPMI 1640 supplemented with 10% FBS and 1% penicillin-streptomycin. For islet dispersion experiments, isolated islets were incubated overnight and dissociated with Accutase (Corning). Dispersed cells were plated onto glass coverslips and cultured on islet medium.

Human islet studies

Human islets from 6 non-diabetic donors (age 25-57 years old, BMI 23.6-33.5 kg/m^2) were obtained through the Integrated Islet Distribution Program (IIDP) via NIH-approved centers. Islets were cultured in PIM(S) media supplemented with 5% human serum (Prodo).

Glucose tolerance tests and GSIS assays

MIN6 cells were incubated in 1 mM glucose Krebs-Ringer-HEPES (KRH) buffer (129 mM NaCl, 5 mM $NaHCO_3$, 4.8 mM KCl, 1.2 mM KH_2PO_4, 1.2 mM $MgSO_4$, 1.2 mM $MgSO_4$, 2.5 mM $CaCl_2$, 10 mM HEPES pH 7.4, 0.1% BSA) for 1h, then transferred to 20 mM glucose for 1h. For islet GSIS, after overnight culture in 5.5 mM glucose RPMI, groups of 6 similar size islets were incubated for 1h in 2.8 mM glucose KRH buffer, and then subjected to 2.8 mM and 16.8 mM glucose stimulation, and supernantants collected. For total insulin content, islets were transferred to high salt buffer (2.15 M NaCl, 10 mM NaH_2PO_4, 40 mM Na_2HPO_4, 1.8 mM EDTA pH 7.4), and sonicated during 2 minutes in a Bioruptor sonicator (Diagenode). Insulin in

supernatant was detected by ELISA (Mercodia). Total islet DNA content was determined by qPCR using standards. Glucose tolerance tests were performed as previously described (10).

Cell Lines and Lentivirus

Culture of insulinoma-derived MIN6 cells, and lentivirus generation with the use of 293T cells was performed as described (61). For generation of a MIN6 cell line expressing a transcriptional transactivator (MIN6-rTTA3), cells were transduced with lentivirus obtained with the pLenti CMV rtTA3 Blast vector (Addgene #26429), and blasticidin (5 μg/ml) selection. Vectors for shRNA mediated knockdown of *Mafa* or *Kat2b* were generated by cloning targeting sequences (Supplemental Table 2) into pLKO.1-TRC cloning vector (Addgene #10879). To generate stable MIN6-rTTA3 cells for doxycycline-mediated expression of N1ΔE-myc or luciferase, N1ΔE cDNA was cloned from pCS2 Notch1 ΔEMV-6MT (Addgene #41737) into pLVX-Tight-Puro vector (Clontech) with pLVX-Tight-Luc (Clontech) used as a negative control. Lentiviral particles generated from these vectors were transduced into MIN6-rTTA3 cells, which were selected with 1 μg/ml puromycin (Sigma). MIN6 cells stably expressing DNMAML-GFP or GFP control were generated after lentivirus infection and FACS-sorting. All vectors used in this study can be found in Supplemental Table 3.

Lentivirus-mediated transduction

Lentivirus were generated in 293T cells as previously described (61). Titration was performed by qPCR. Intact or dispersed islets were transduced with 10 transducing units (TU)/cell, assuming that an average islet contains 1000 cells, in complete medium enriched with 8 μg/ml sequabrene (Sigma). Imaging and GSIS experiments in human islets were performed 96h after lentivirus infection.

Western blotting and quantitative PCR

Lysates were resolved by SDS-PAGE, followed by Western blot and visualization using the ECL Western Blotting Detection kit (GE Healthcare Bio-Sciences). RNA was isolated with Trizol (Thermo Fisher), cDNA was obtained with the High-Capacity cDNA Reverse Transcription Kit (Thermo Fisher) and qPCR performed using Power SYBR Master Mix (Thermo Fisher). Primers sequences used are detailed in Supplemental Table 2.

Immunofluorescence, β Cell Mass Determination, BrdU and TUNEL Assay

Tissue was fixed in 4% paraformaldehyde/PBS at 4ºC for 2-4h, followed by overnight incubation in 30% sucrose/PBS. Tissue was embedded in OCT-compound and flash frozen in dry ice-chilled isopentane. 5 µM thick tissue sections were processed according to standard procedures. For MafA and Hes1 immunostaining, slides were incubated for 20 minutes at 70ºC with HistoVT One (Nacalai) for antigen retrieval. For BrdU staining, mice were injected intraperitoneally with 100 mg/kg BrdU (Millipore-Sigma) 5h before sacrifice. After standard processing of the tissue, slides were incubated at 37ºC in 2N HCl for 30 min, followed by incubation in 0.1 M sodium borate buffer pH 8.5 for 10 min, prior to incubation in primary antibodies, then donkey secondary antibodies (Jackson ImmunoResearch), both diluted in PBS containing 5% normal donkey serum, 1% BSA and 0.1% Triton X-100. TUNEL assay was performed with the *In Situ* Cell Death Detection Kit, Fluorescein (Roche Applied Sciences) following the instructions from the manufacturer, and pancreas sections further stained with insulin and DAPI. β cell mass analyses, and immunofluorescence in MIN6 cells, dispersed or intact islets was performed as previously described (60).

Confocal microscopy

For confocal microscopy assays, Axio Observer Z1 with LSM 710 scanning module was used (Zeiss). Images were obtained with an 40 × Zeiss Plan-Apochromat oil objective. Imaging was performed in a single confocal microscopy session for each experiment. For each session, the

photomultiplier voltage settings (below 600V), and laser transmission (≤ 2%) for each fluorophore, were determined to maximize the dynamic range of the signal. Controls were used for each experiment to confirm specific signals. All images were obtained in a 1024 × 1024 pixel format. For microscope operation and image gathering, ZEN (Zeiss) software was used.

Quantification of immunofluorescence experiments

Quantitative analysis of fluorescence intensity for nuclear antigens (MafA, Pdx1 or Hes1) was performed with images gathered from pancreas tissue slides. For this, raw multichannel LSM files were processed in NIH ImageJ software (http://rsb.info.nih.gov/ij/index.htm), and the channel of interest subjected to background correction using the "rolling ball" algorithm implemented in ImageJ. The region of interested (ROI) was then drawn on 20-30 random nuclei per image, while visualizing the insulin channel to select β cells. The signal intensity for the ROI of the channel of interest (nuclear staining) was obtained per image, and then averaged per pancreas (5-10 images per pancreas). Results shown are the average of 3-6 mice per group. The average pixel intensity values were referenced to the values obtained for the control of each experiment, and expressed as arbitrary units (AU). For qualitative analysis (Ki67, BrdU, MafA expression in vitro), a threshold was set using the *Threshold* function of ImageJ, and positive and negative cells were counted. Images were processed with ZEN2, the only manipulation performed was linear contrast stretching to attain the optimal dynamic signal range for each set of images. Representative pictures shown for these experiments have quantified values approximated to the final average.

Transmission Electron Microscopy

Islets were isolated with 0.1 mg/ml Liberase TL (Roche) and handpicked in Hank's balanced salt solution (HBSS) containing 0.2% BSA and 2.8 mM glucose. Isolated islets were immediately fixed at 4ºC for 3h with 2% paraformaldehyde, 2.5% glutaraldehyde and 3 μM $CaCl_2$ in 0.1M

sodium cacodylate buffer pH 7.4. Samples were processed as described (62). For quantification analyses, the area occupied by insulin vesicles and β cell cytoplasmic area was measured with ImageJ in 50-60 images per mouse.

Islet diameter

Freshly isolated islets were maintained in ice cold RPMI with 2% normal calf serum, and images were gathered with an Olympus IX70 microscope. Individual islet area was determined using ImageJ, and results converted to diameter.

Statistical Analysis

Results are shown as mean ± SEM. Differences between 2 groups were calculated using a 2-sided Student's t test, ratio paired Student's t test or Mann-Whitney U test as indicated. Differences between multiple groups and a control were calculated by one-way ANOVA followed by Dunnett's multiple comparisons post-hoc test. A P value of less than 0.05 was considered statistically significant.

Study approval

The Columbia University Institutional Animal Care and Utilization Committee approved all animal procedures. Human islets were harvested from deceased donors without any identifying information. Informed consent and IRB approval was obtained at islet isolation centers.

AUTHOR CONTRIBUTIONS

A.B. conducted experiments and contributed to the experimental design, discussion, and writing of the manuscript. C.Z conducted experiments and contributed to the review and editing of the manuscript. L.S. contributed to the experimental design, discussion, and review and editing of the manuscript. U.P. contributed to the experimental design, discussion and writing of the manuscript.

ACKNOWLEDGEMENTS

We thank A. Flete and T. Kolar for excellent technical support, as well as members of the Pajvani and Accili laboratories for insightful discussion. This work was supported by NIH DK103818 (UBP), a Russell Berrie Foundation Award (ABH) and an American Diabetes Association Grant 1-17-PMF-025 (ABH). These studies used the resources of the Diabetes and Endocrinology Research Center Flow Core Facility funded in part through Center Grant 5P30DK063608.

REFERENCES

1. Alejandro EU, Gregg B, Blandino-Rosano M, Cras-Méneur C, Bernal-Mizrachi E. Natural history of β-cell adaptation and failure in type 2 diabetes. *Mol. Aspects Med.* 2015;42:19–41.

2. Butler AE et al. Beta-cell deficit and increased beta-cell apoptosis in humans with type 2 diabetes. *Diabetes* 2003;52(1):102–110.

3. Talchai C, Xuan S, Lin HV, Sussel L, Accili D. Pancreatic β Cell Dedifferentiation as a Mechanism of Diabetic β Cell Failure. *Cell* 2012;150(6):1223–1234.

4. Apelqvist A et al. Notch signalling controls pancreatic cell differentiation. *Nature* 1999;400(6747):877–881.

5. Jensen J et al. Control of endodermal endocrine development by Hes-1. *Nat Genet* 2000;24(1):36–44.

6. Fujikura J et al. Notch/Rbp-j signaling prevents premature endocrine and ductal cell differentiation in the pancreas. *Cell Metab* 2006;3(1):59–65.

7. Murtaugh LC, Stanger BZ, Kwan KM, Melton DA. Notch signaling controls multiple steps of pancreatic differentiation. *Proc Natl Acad Sci USA* 2003;100(25):14920–14925.

8. Zeggini E et al. Meta-analysis of genome-wide association data and large-scale replication identifies additional susceptibility loci for type 2 diabetes. *Nat Genet* 2008;40(5):638–645.

9. Valenti L et al. Hepatic notch signaling correlates with insulin resistance and nonalcoholic fatty liver disease. *Diabetes* 2013;62(12):4052–4062.

10. Pajvani UB et al. Inhibition of Notch signaling ameliorates insulin resistance in a FoxO1-dependent manner. *Nat Med* 2011;17(8):961–967.

11. Pajvani UB et al. Inhibition of Notch uncouples Akt activation from hepatic lipid accumulation by decreasing mTorc1 stability. *Nat Med* 2013;19(8):1054–1060.

12. Duncan AW et al. Integration of Notch and Wnt signaling in hematopoietic stem cell maintenance. *Nat. Immunol.* 2005;6(3):314–322.

13. Nowotschin S, Xenopoulos P, Schrode N, Hadjantonakis A-K. A bright single-cell resolution live imaging reporter of Notch signaling in the mouse. *BMC Dev. Biol.* 2013;13:15.

14. Kopinke D et al. Lineage tracing reveals the dynamic contribution of Hes1+ cells to the developing and adult pancreas. *Development* 2011;138(3):431–441.

15. Billiard F et al. Delta-like Ligand-4-Notch Signaling Inhibition Regulates Pancreatic Islet Function and Insulin Secretion. *Cell Rep* 2018;22(4):895–904.

16. Herrera PL. Adult insulin- and glucagon-producing cells differentiate from two independent cell lineages. *Development* 2000;127(11):2317–2322.

17. Tamarina NA, Roe MW, Philipson L. Characterization of mice expressing Ins1 gene promoter driven CreERT recombinase for conditional gene deletion in pancreatic β-cells. *Islets*

2014;6(1):e27685.

18. Kopan R, Schroeter EH, Weintraub H, Nye JS. Signal transduction by activated mNotch: importance of proteolytic processing and its regulation by the extracellular domain. *Proc Natl Acad Sci USA* 1996;93(4):1683–1688.

19. Han S-I, Aramata S, Yasuda K, Kataoka K. MafA stability in pancreatic beta cells is regulated by glucose and is dependent on its constitutive phosphorylation at multiple sites by glycogen synthase kinase 3. *Mol Cell Biol* 2007;27(19):6593–6605.

20. Rocques N et al. GSK-3-mediated phosphorylation enhances Maf-transforming activity. *Mol Cell* 2007;28(4):584–597.

21. Guo S et al. The stability and transactivation potential of the mammalian MafA transcription factor are regulated by serine 65 phosphorylation. *J Biol Chem* 2009;284(2):759–765.

22. Kurooka H, Honjo T. Functional interaction between the mouse notch1 intracellular region and histone acetyltransferases PCAF and GCN5. *J Biol Chem* 2000;275(22):17211–17220.

23. Klochendler A et al. The Genetic Program of Pancreatic β-Cell Replication In Vivo. *Diabetes* 2016;65(7):2081–2093.

24. Eychène A, Rocques N, Pouponnot C. A new MAFia in cancer. *Nat Rev Cancer* 2008;8(9):683–693.

25. Raum JC et al. FoxA2, Nkx2.2, and PDX-1 regulate islet beta-cell-specific mafA expression through conserved sequences located between base pairs -8118 and -7750 upstream from the transcription start site. *Mol Cell Biol* 2006;26(15):5735–5743.

26. Oropeza D et al. Phenotypic Characterization of MIP-CreERT1Lphi Mice With Transgene-Driven Islet Expression of Human Growth Hormone. *Diabetes* 2015;64(11):3798–3807.

27. Tschen S-I, Dhawan S, Gurlo T, Bhushan A. Age-dependent decline in beta-cell proliferation restricts the capacity of beta-cell regeneration in mice. *Diabetes* 2009;58(6):1312–1320.

28. Puri S, Akiyama H, Hebrok M. VHL-mediated disruption of Sox9 activity compromises β-cell identity and results in diabetes mellitus. *Genes Dev* 2013;27(23):2563–2575.

29. Sasson A et al. Islet Pericytes Are Required for β-Cell Maturity. *Diabetes* 2016;65(10):3008–3014.

30. Cras-Méneur C, Conlon M, Zhang Y, Pasca Di Magliano M, Bernal-Mizrachi E. Early pancreatic islet fate and maturation is controlled through RBP-Jκ. *Sci Rep* 2016;6:26874.

31. Landsman L, Parent A, Hebrok M. Elevated Hedgehog/Gli signaling causes beta-cell dedifferentiation in mice. *Proc Natl Acad Sci USA* 2011;108(41):17010–17015.

32. Szabat M et al. Reduced Insulin Production Relieves Endoplasmic Reticulum Stress and Induces β Cell Proliferation. *Cell Metab* 2016;23(1):179–193.

33. Bar Y, Russ HA, Knoller S, Ouziel-Yahalom L, Efrat S. HES-1 is involved in adaptation of adult human beta-cells to proliferation in vitro. *Diabetes* 2008;57(9):2413–2420.

34. Bar Y et al. Redifferentiation of expanded human pancreatic β-cell-derived cells by inhibition of the NOTCH pathway. *J Biol Chem* 2012;287(21):17269–17280.

35. van der Meulen T et al. Virgin Beta Cells Persist throughout Life at a Neogenic Niche within Pancreatic Islets. *Cell Metab* 2017;25(4):911–926.e6.

36. Hang Y et al. The MafA transcription factor becomes essential to islet β-cells soon after birth. *Diabetes* 2014;63(6):1994–2005.

37. Kitamura YI et al. FoxO1 protects against pancreatic beta cell failure through NeuroD and MafA induction. *Cell Metab* 2005;2(3):153–163.

38. Zhang C et al. MafA is a key regulator of glucose-stimulated insulin secretion. *Mol Cell Biol* 2005;25(12):4969–4976.

39. Nishimura W, Bonner-Weir S, Sharma A. Expression of MafA in pancreatic progenitors is detrimental for pancreatic development. *Dev. Biol.* 2009;333(1):108–120.

40. Aguayo-Mazzucato C et al. Mafa expression enhances glucose-responsive insulin secretion in neonatal rat beta cells. *Diabetologia* 2011;54(3):583–593.

41. Hamze Z et al. Altered MENIN expression disrupts the MAFA differentiation pathway in insulinoma. *Endocr Relat Cancer* 2013;20(6):833–848.

42. Pechhold S et al. Transcriptional analysis of intracytoplasmically stained, FACS-purified cells by high-throughput, quantitative nuclease protection. *Nat Biotechnol* 2009;27(11):1038–1042.

43. Banerjee RR et al. Gestational Diabetes Mellitus From Inactivation of Prolactin Receptor and MafB in Islet β-Cells. *Diabetes* 2016;65(8):2331–2341.

44. Nishimura W et al. A switch from MafB to MafA expression accompanies differentiation to pancreatic beta-cells. *Dev. Biol.* 2006;293(2):526–539.

45. Artner I et al. MafA and MafB regulate genes critical to beta-cells in a unique temporal manner. *Diabetes* 2010;59(10):2530–2539.

46. Hagman DK, Hays LB, Parazzoli SD, Poitout V. Palmitate inhibits insulin gene expression by altering PDX-1 nuclear localization and reducing MafA expression in isolated rat islets of Langerhans. *J Biol Chem* 2005;280(37):32413–32418.

47. Harmon JS, Stein R, Robertson RP. Oxidative stress-mediated, post-translational loss of MafA protein as a contributing mechanism to loss of insulin gene expression in glucotoxic beta cells. *J Biol Chem* 2005;280(12):11107–11113.

48. Matsuoka T-A et al. Regulation of MafA expression in pancreatic beta-cells in db/db mice with diabetes. *Diabetes* 2010;59(7):1709–1720.

49. Bader E et al. Identification of proliferative and mature β-cells in the islets of Langerhans. *Nature* 2016;535(7612):430–434.

50. Rui J et al. β Cells that Resist Immunological Attack Develop during Progression of

Autoimmune Diabetes in NOD Mice. *Cell Metab* 2017;25(3):727–738.

51. Avrahami D et al. Aging-Dependent Demethylation of Regulatory Elements Correlates with Chromatin State and Improved β Cell Function. *Cell Metab* 2015;22(4):619–632.

52. Bi P et al. Inhibition of Notch signaling promotes browning of white adipose tissue and ameliorates obesity. *Nat Med* 2014;20(8):911–918.

53. Li J, Tang Y, Cai D. IKKβ/NF-κB disrupts adult hypothalamic neural stem cells to mediate a neurodegenerative mechanism of dietary obesity and pre-diabetes. *Nat Cell Biol* 2012;14(10):999–1012.

54. Fukuda D et al. Notch ligand delta-like 4 blockade attenuates atherosclerosis and metabolic disorders. *Proc Natl Acad Sci USA* 2012;109(27):E1868–77.

55. Jeon JH, Suh HN, Kim MO, Ryu JM, Han HJ. Glucosamine-induced OGT activation mediates glucose production through cleaved Notch1 and FoxO1, which coordinately contributed to the regulation of maintenance of self-renewal in mouse embryonic stem cells. *Stem Cells Dev.* 2014;23(17):2067–2079.

56. Song N-J et al. Notch1 deficiency decreases hepatic lipid accumulation by induction of fatty acid oxidation. *Sci Rep* 2016;6:19377.

57. Kim K et al. γ-Secretase Inhibition Lowers Plasma Triglyceride-Rich Lipoproteins by Stabilizing the LDL Receptor. *Cell Metab* 2018;27(4):816–827.e4.

58. Groth C, Fortini ME. Therapeutic approaches to modulating Notch signaling: current challenges and future prospects. *Semin. Cell Dev. Biol.* 2012;23(4):465–472.

59. Maillard I et al. Mastermind critically regulates Notch-mediated lymphoid cell fate decisions. *Blood* 2004;104(6):1696–1702.

60. Bartolomé A et al. Pancreatic β-cell failure mediated by mTORC1 hyperactivity and autophagic impairment. *Diabetes* 2014;63(9):2996–3008.

61. Bartolomé A, Guillén C, Benito M. Autophagy plays a protective role in endoplasmic reticulum stress-mediated pancreatic β cell death. *Autophagy* 2012;8(12):1757–1768.

62. Koyanagi M et al. Ablation of TSC2 Enhances Insulin Secretion by Increasing the Number of Mitochondria through Activation of mTORC1. *PLoS ONE* 2011;6(8):e23238.

Figure 1

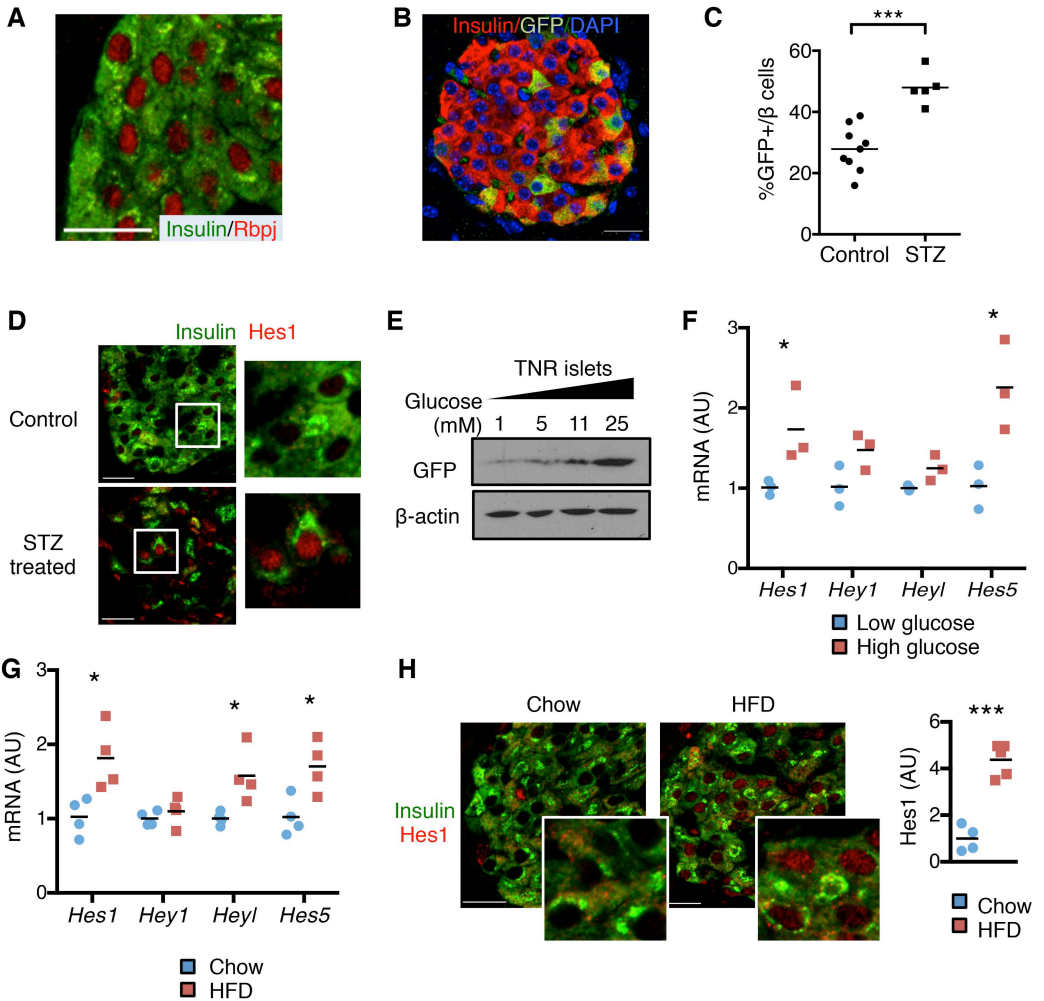

Figure 1. Increased Notch activity with β cell stress

(A) Representative image of pancreatic sections from wild-type (WT) mice stained with antibodies directed against insulin and Rbpj.

(B) Representative image of pancreatic sections from Transgenic Notch Reporter (TNR) mice.

(C) Quantitation of %GFP+ cells in remaining β cells from TNR mice after low-dose STZ (N=5-9 mice/group).

(D) Representative images of pancreatic sections stained with antibodies directed against Hes1 and insulin in vehicle (Control) and STZ-treated TNR mice (N=5-9 mice/group).

(E) Western blots from islets isolated from TNR mice, incubated for 15h in medium containing indicated glucose concentrations. Representative blots from 2 experiments.

(F) Gene expression in islets isolated from WT mice, cultured overnight in medium containing low (1 mM) or high (25 mM) glucose (N=3 biologic replicates).

(G) Gene expression in islets isolated from 24-week high-fat diet (HFD)-fed WT mice, as compared to normal chow diet-fed littermate controls (N=5 mice/group).

(H) Representative images of pancreatic sections stained with antibodies directed against Hes1 and insulin, with quantitation of nuclear Hes1 fluorescence intensity in β cells (N=4-5 mice/group).

Scale bars: 20 μm. All data are shown with group means; *, $P < 0.05$, **, $P < 0.01$, ***, $P < 0.001$ by two-tailed *t* test.

Figure 2

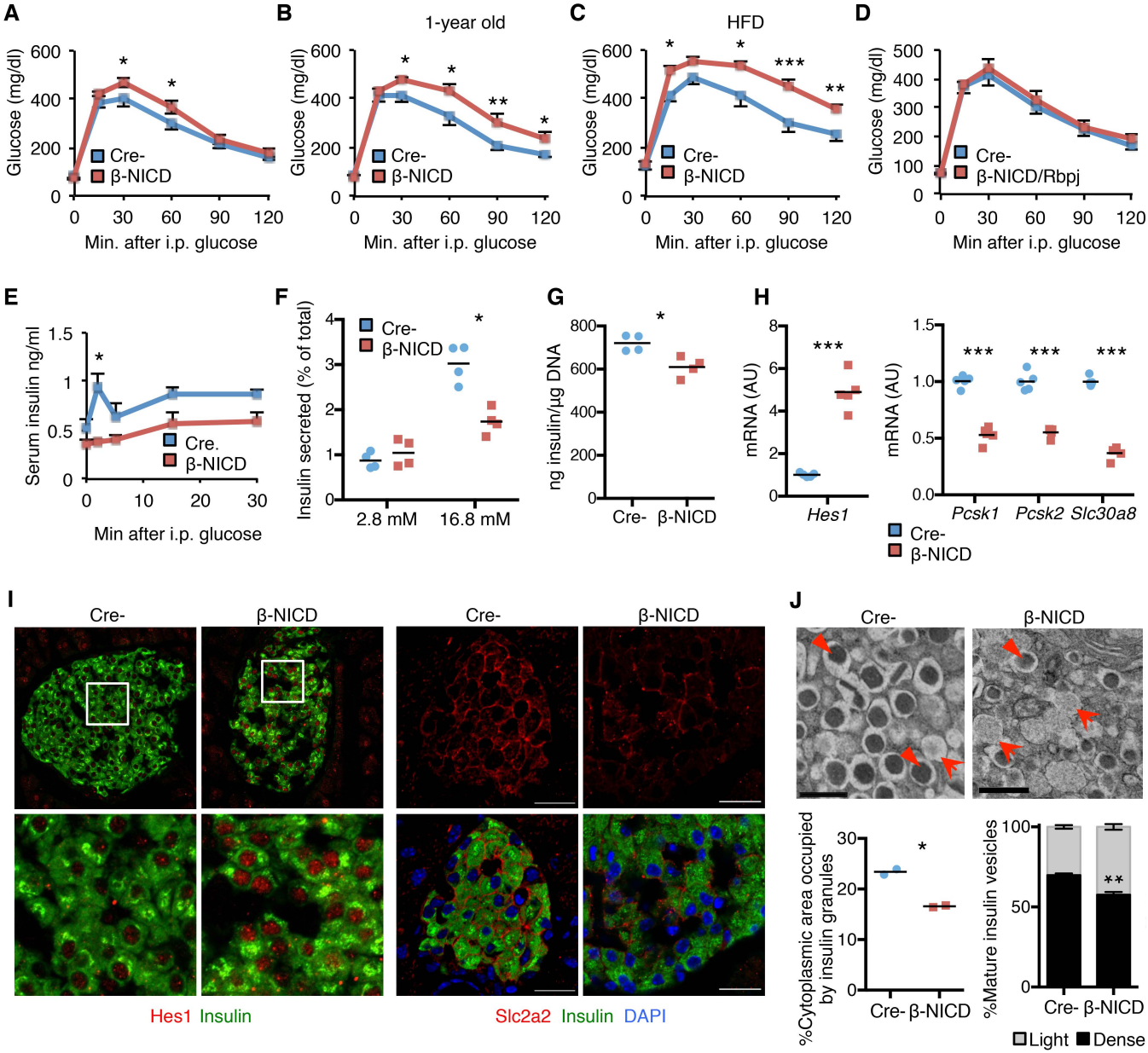

Figure 2. β cell Notch activation prevents normal GSIS, leading to glucose intolerance

(A) Glucose tolerance test (GTT) in chow-fed, adult β-NICD and Cre- control mice (N=7-8 mice/group).

(B) GTT in chow-fed, 1 year-old β-NICD mice and Cre- control mice (N=7-8 mice/group).

(C) GTT in β-NICD and Cre- control mice fed HFD for 8 weeks (N=8-10 mice/group).

(D) GTT in chow-fed, adult β-NICD/Rbpj and Cre- control mice (N=7 mice/group).

(E) Plasma insulin post-intraperitoneal glucose injection in chow-fed β-NICD and Cre- control mice (N=5 mice/group)

(F) Glucose-stimulated insulin secretion (GSIS) in islets isolated from β-NICD and Cre- control mice, adjusted for islet insulin content (N=4 mice/group).

(G) Insulin content in islets isolated from β-NICD and Cre- control mice, adjusted for islet DNA content (N=4 mice/group).

(H) Gene expression in islets isolated from chow-fed β-NICD and Cre- control mice (N=5 mice/group).

(I) Representative images of pancreatic sections from β-NICD and Cre- control mice stained with antibodies directed against Hes1 (left) or Slc2a2 (right), (N=5 mice/group). Scale bars: 20 µm.

(J) Representative electron micrographs from 1-year-old β-NICD mice and Cre- control mice (top) with arrows representing immature vesicles and arrowheads, mature vesicles, scale bars: 500 nm. Quantitation of mature (over total) dense-core insulin vesicles (bottom left) and cytoplasmic area occupied by insulin vesicles (bottom right) (N=2 mice/group).

All data are shown with group means ± s.e.m.; *, $P < 0.05$, **, $P < 0.01$, ***, $P < 0.001$ by two-tailed *t* test.

Figure 3

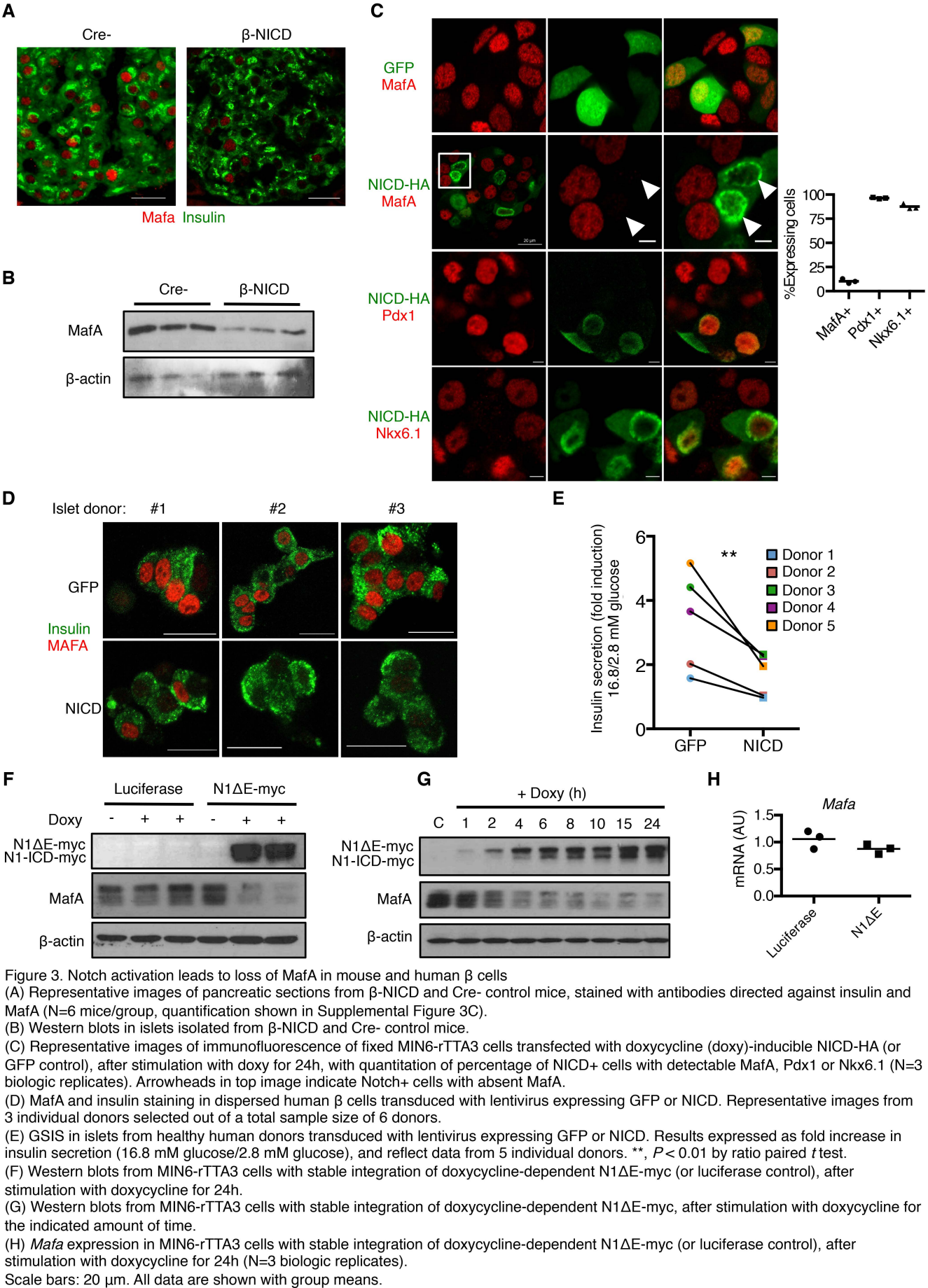

Figure 3. Notch activation leads to loss of MafA in mouse and human β cells

(A) Representative images of pancreatic sections from β-NICD and Cre- control mice, stained with antibodies directed against insulin and MafA (N=6 mice/group, quantification shown in Supplemental Figure 3C).

(B) Western blots in islets isolated from β-NICD and Cre- control mice.

(C) Representative images of immunofluorescence of fixed MIN6-rTTA3 cells transfected with doxycycline (doxy)-inducible NICD-HA (or GFP control), after stimulation with doxy for 24h, with quantitation of percentage of NICD+ cells with detectable MafA, Pdx1 or Nkx6.1 (N=3 biologic replicates). Arrowheads in top image indicate Notch+ cells with absent MafA.

(D) MafA and insulin staining in dispersed human β cells transduced with lentivirus expressing GFP or NICD. Representative images from 3 individual donors selected out of a total sample size of 6 donors.

(E) GSIS in islets from healthy human donors transduced with lentivirus expressing GFP or NICD. Results expressed as fold increase in insulin secretion (16.8 mM glucose/2.8 mM glucose), and reflect data from 5 individual donors. **, $P < 0.01$ by ratio paired *t* test.

(F) Western blots from MIN6-rTTA3 cells with stable integration of doxycycline-dependent N1ΔE-myc (or luciferase control), after stimulation with doxycycline for 24h.

(G) Western blots from MIN6-rTTA3 cells with stable integration of doxycycline-dependent N1ΔE-myc, after stimulation with doxycycline for the indicated amount of time.

(H) *Mafa* expression in MIN6-rTTA3 cells with stable integration of doxycycline-dependent N1ΔE-myc (or luciferase control), after stimulation with doxycycline for 24h (N=3 biologic replicates).

Scale bars: 20 μm. All data are shown with group means.

Figure 4

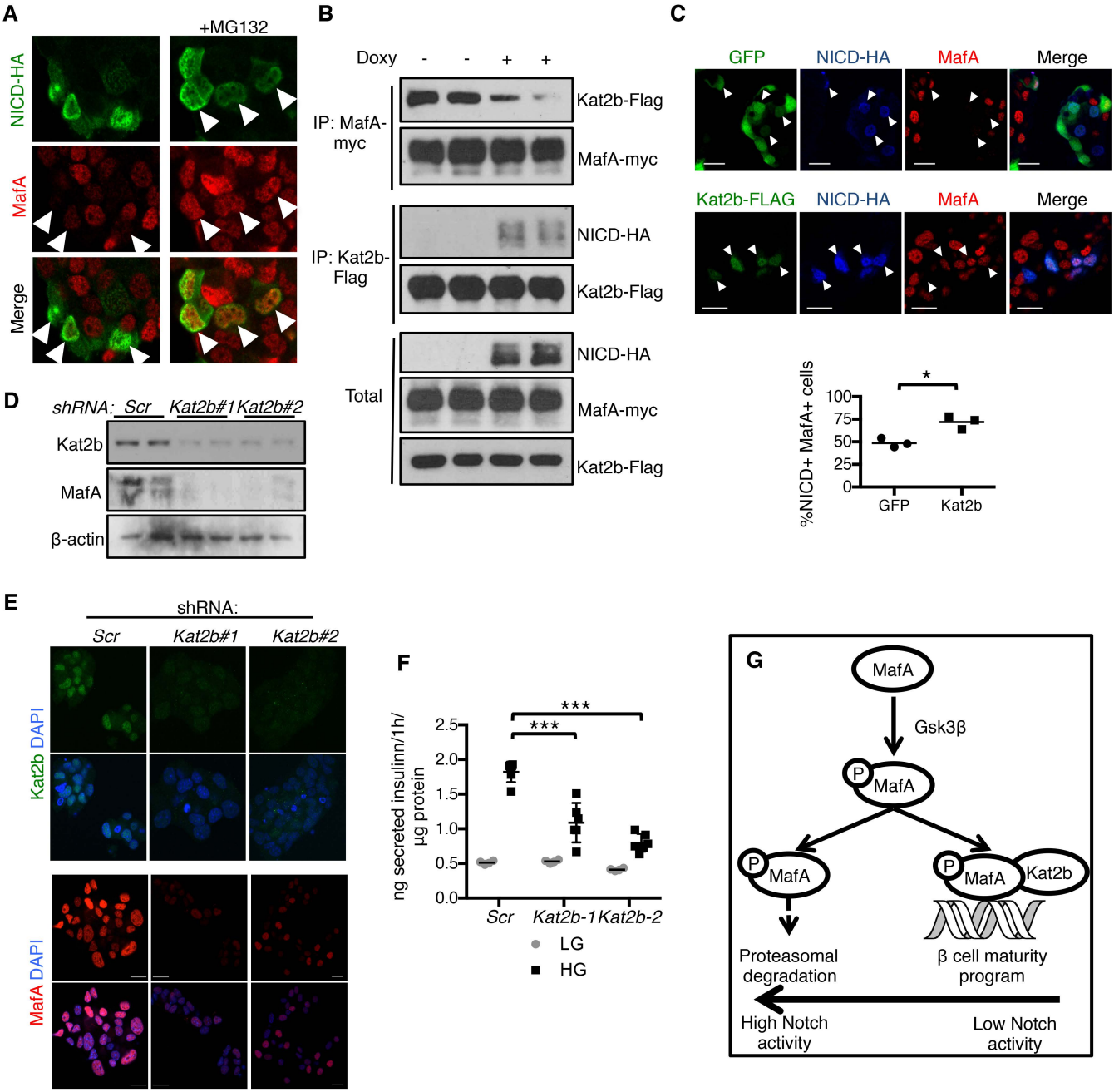

Figure 4. Notch causes MafA degradation by preventing its association with Kat2b.
(A) Representative immunofluorescence images of fixed MIN6 cells transiently transfected with NICD-HA, with or without MG132. (N=4 independent experiments)
(B) Western blots from immunoprecipitates derived from 293T cells with stable integration of the rTTA3 transcriptional trans-activator, transfected with MafA-myc, Kat2b-Flag and Tet-On NICD-HA, with or without stimulation with doxycycline for 4h.
(C) Representative images of immunofluorecescence of fixed MIN6-rTTA3 cotransfected with Tet-On NICD-HA and GFP or Kat2b-Flag, after stimulation with doxy for 8h, and quantitation of percentage of NICD+/GFP+ or NICD+/Kat2b+ (arrowheads) cells with detectable MafA (N=3 independent experiments, ~250 cells analyzed per sample); *, $P < 0.05$ by two-tailed *t* test.
(D) Western blots from MIN6 cells transduced with lentivirus encoding shRNA targeting *Kat2b* (2 different sequences: #1 and #2) or scrambled control (Scr).
(E) Immunofluorescence images of fixed MIN6 cells transduced with lentivirus encoding shRNA targeting *Kat2b*, or scrambled shRNA (Scr). Representative images from 2 independent experiments.
(F) GSIS from MIN6 cells transduced with lentivirus encoding shRNA against *Kat2b* or scrambled control (Scr), in medium containing low (1 mM, LG) or high (25 mM, HG) glucose. Results from a representative experiment with 6 replicates per condition, the experiment was performed 3 times; ***, $P < 0.001$ by one-way ANOVA and Dunnett's multiple comparisons post-hoc test.
(G) Model of Notch regulation of MafA-Kat2b interaction and MafA proteasomal degradation.
Scale bars: 20 µm. All data are shown with group means.

Figure 5

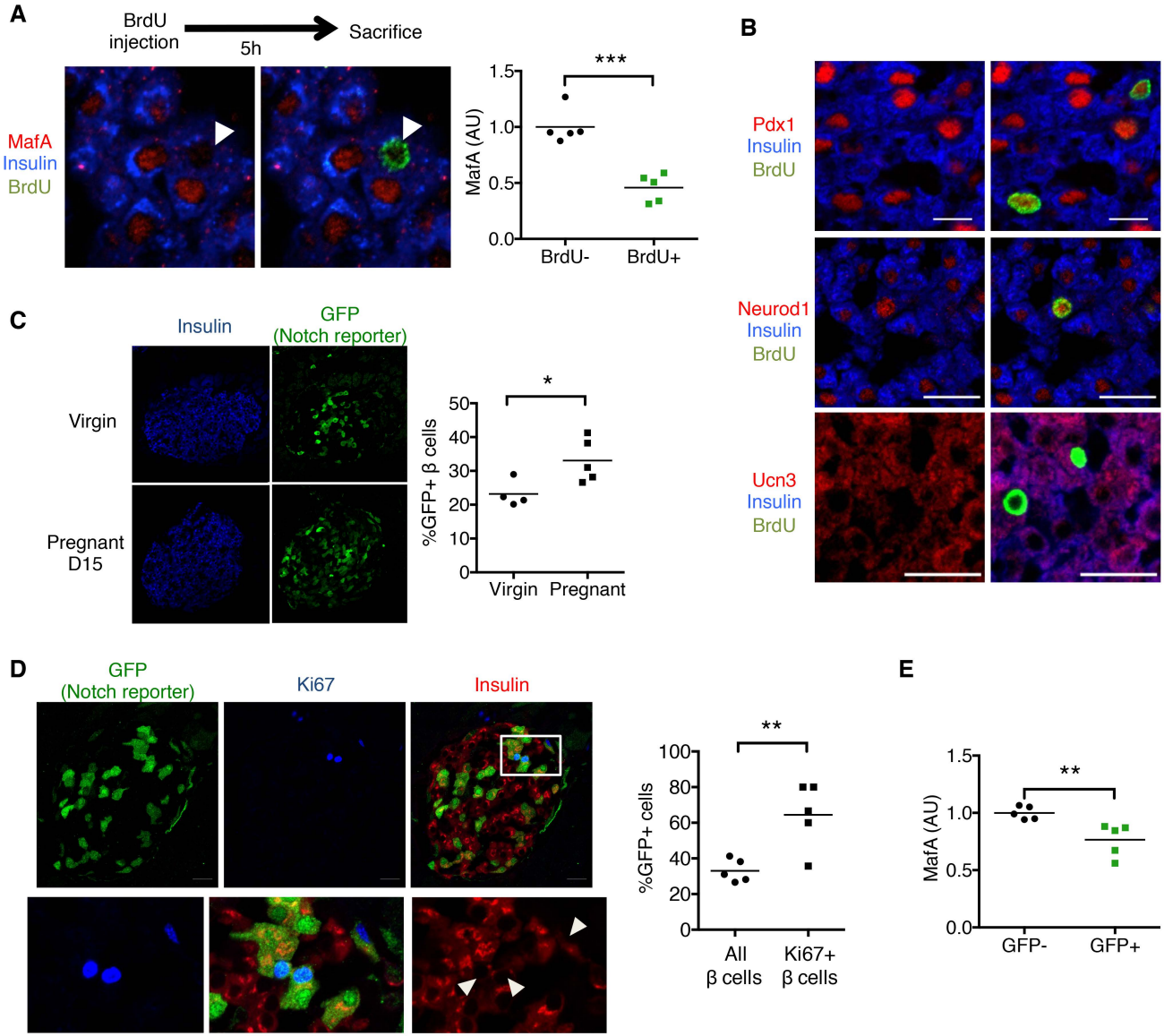

Figure 5. Notch activation and reduced maturity in proliferating β cells.
(A) Representative images of pancreatic sections from pregnant (D15) WT mice, and quantitation expressed as average MafA fluorescence intensity of BrdU+ and BrdU- populations (N=5 mice/group). Individual cells are plotted in Supplemental Figure 6A.
(B) Representative image of pancreatic sections from pregnant (D15) mice stained for BrdU as well as antibodies directed against insulin and Pdx1, Neurod1 or Ucn3 (N=5 mice/group).
(C) Representative images of pancreatic sections from virgin and pregnant (D15) TNR mice, with quantitation of %GFP+ β cells (N=4-5 mice/group).
(D) Representative images of pancreatic sections from pregnant (D15) TNR mice showing Ki67, insulin and GFP reporter staining (top), with increased magnification of the boxed region (bottom); arrows indicate Ki67+ β cells. Quantitation of %GFP+ β cells or %GFP+ Ki67+ β cells (N=5 mice/group; overall count of 3995 total β cells and 188 Ki67+ β cells).
(E) Quantitation of average MafA fluorescence intensity in GFP- and GFP+ β cells from chow-fed TNR mice, normalized to average value in GFP- cells (N=5 mice). Approximately 1000 cells quantified per pancreas.
Scale bars: 20 μm. All data are shown with group means; *, $P < 0.05$, **, $P < 0.01$, ***, $P < 0.001$ by two-tailed *t* test.

Figure 6

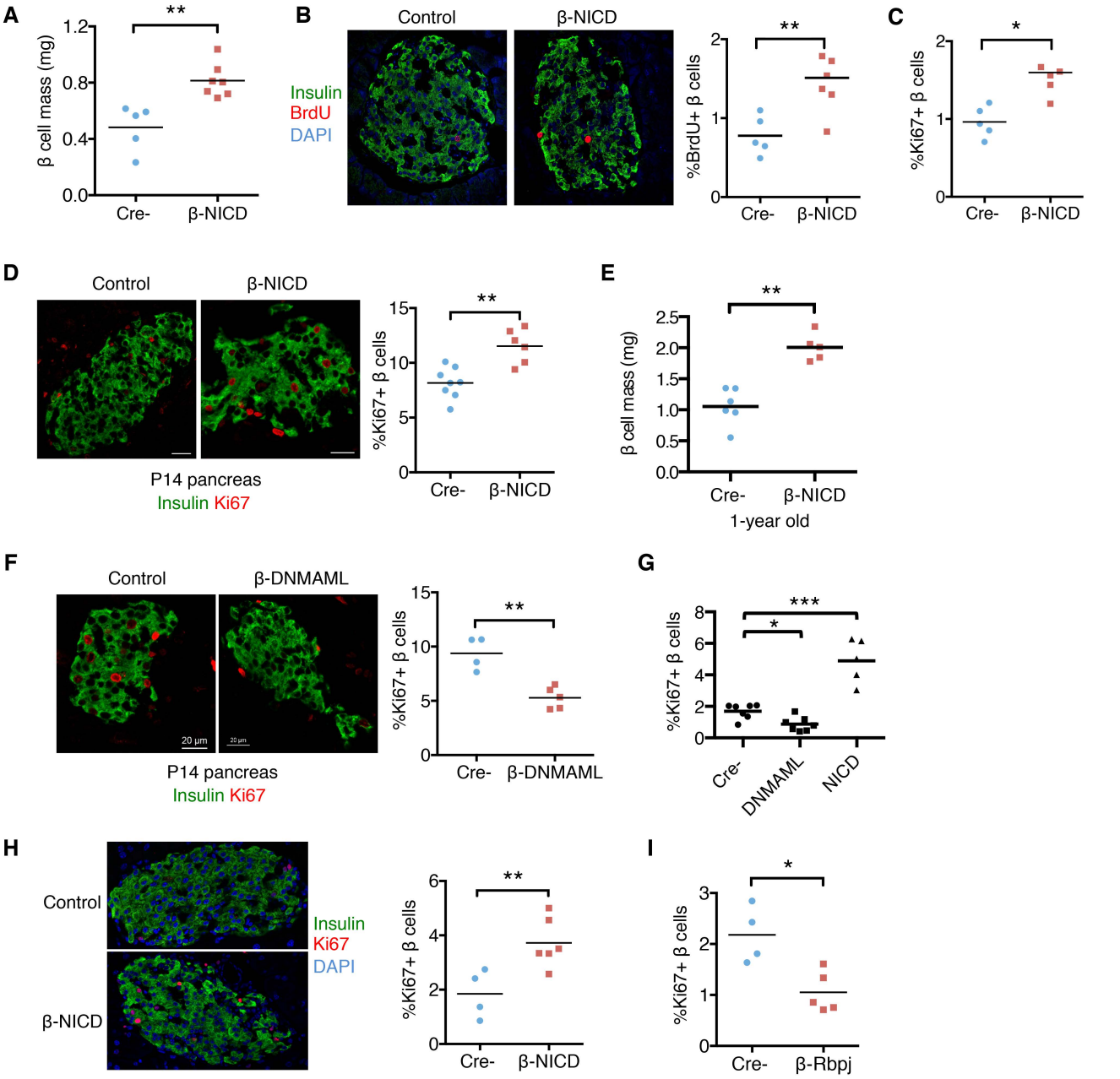

Figure 6. Notch activation increases β cell proliferative capacity.
(A) Quantitation of β cell mass in adult β-NICD and Cre- control mice (N=5-7 mice/group); *, $P < 0.05$ by two-tailed *t* test.
(B) Representative images and quantitation of BrdU+ β cells in pancreatic sections from adult β-NICD and Cre- control mice (N=5 mice/group); **, $P < 0.01$ by two-tailed *t* test.
(C) Quantitation of Ki67+ β cells in pancreatic sections from adult β-NICD and Cre- control mice (N=5 mice/group); *, $P < 0.05$ by two-tailed *t* test.
(D) Representative images and quantitation of Ki67+ β cells in postnatal day 14 (P14) pancreas in β-NICD and Cre- control mice (N=6-8 mice/group); **, $P < 0.01$ by two-tailed *t* test.
(E) Quantitation of β cell mass in 1-year old β-NICD and Cre- mice (N=5-6 mice/group); **, $P < 0.01$ by two-tailed *t* test.
(F) Representative images and quantitation of Ki67+ β cells in P14 pancreas in β-DNMAML and Cre- control mice (N=4-5 mice/group); **, $P < 0.01$ by two-tailed *t* test.
(G) Quantitation of Ki67+ Pdx1+ cells in islet cells dispersed from control (*MIP-Cre-*), DNMAML1 (*MIP-Cre^{ERT}+; R26-DNMAML/+*), or NICD (*MIP-Cre^{ERT}+; R26-NICD/+*) mice, grown in full medium containing 22 mM glucose and 1 μM 4-OHT for 4 days (N=5-7 mice/group); *, $P < 0.05$, ***, $P < 0.001$ by one-way ANOVA and Dunnett's multiple comparisons post-hoc test. Representative images are shown in Supplemental Figure 6D.
(H) Representative images and quantitation of Ki67+ β cells in pancreatic sections from pregnant (D15) β-NICD and Cre- control females (N=4-6 mice/group); **, $P < 0.01$ by two-tailed *t* test.
(I) Quantitation of Ki67+ β cells in pancreatic sections of pregnant (D15) β-Rbpj and Cre- control females (N=4-5 mice/group); *, $P < 0.05$ by two-tailed *t* test. Scale bars: 20 μm. All data are shown with group means.

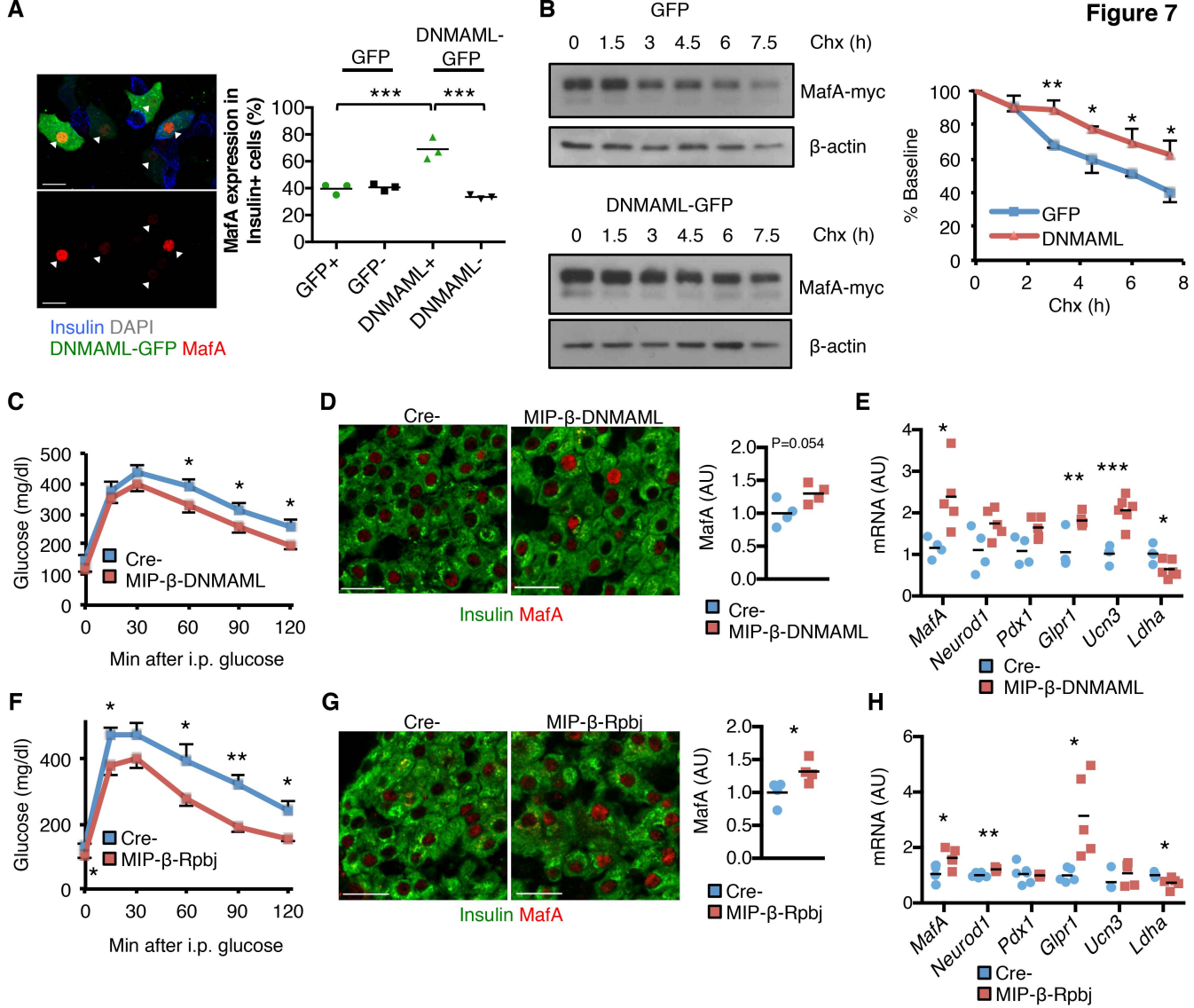

Figure 7. Notch loss-of-function stabilizes β cell MafA and improves glucose tolerance

(A) Representative image of islet cells dispersed from WT mice transduced with lentivirus expressing DNMAML-GFP (or GFP control), and exposed to 100 nM palmitate and 25 mM glucose for 72h. Arrows indicate DNMAML+ cells. Quantitation shows insulin+ MafA+ islet cells in transduced vs. non-transduced cells (N=3 independent experiments); ***, $P < 0.001$ by one-way ANOVA and Dunnett's multiple comparisons post-hoc test.

(B) Western blots, and quantitation of residual MafA-Myc signal expressed as %baseline, from MIN6 cells with stable integration of DNMAML-GFP (or GFP control), transiently transfected with MafA-myc then treated with 10 μg/ml cycloheximide (Chx) for the indicated times (N=3 independent experiments); *, $P < 0.05$, **, $P < 0.01$ by two-tailed *t* test.

(C) GTT in tamoxifen-treated, HFD-fed MIP-β-DNMAML and Cre- control mice (N=9-11 mice/group) as per experimental protocol shown in Supplemental Figure 8C; *, $P < 0.05$ by two-tailed *t* test.

(D) Representative images and quantitation of MafA fluorescence intensity in pancreatic sections from HFD-fed MIP-β-DNMAML and Cre- control mice (N=4 mice/group); $P = 0.054$ by two-tailed *t* test.

(E) Gene expression in islets isolated from HFD-fed MIP-β-DNMAML and Cre- control mice (N=4-5 mice/group); *, $P < 0.05$, **, $P < 0.01$, ***, $P < 0.001$ by two-tailed *t* test.

(F) GTT in HFD-fed MIP-β-Rbpj and Cre- control mice (N=9 mice/group); *, $P < 0.05$, **, $P < 0.01$ by two-tailed *t* test.

(G) Representative images and quantitation of MafA fluorescence intensity in pancreatic sections from HFD-fed MIP-β-Rbpj and Cre- control mice (N=4 mice/group); *, $P < 0.05$ by two-tailed *t* test.

(H) Gene expression in islets isolated from HFD-fed MIP-β-Rbpj and Cre- control mice (N=5-6 mice/group); *, $P < 0.05$, **, $P < 0.01$ by two-tailed *t* test.